Journal of Ceramic Processing Research. Vol. 16, No. 4, pp. 406~410 (2015)

J O U R N A L O F
Ceramic Processing Research

Decoration of MgO nanowires with Gd_2O_3 nanoparticles: structure and photoluminescence properties

Wooseung Kang[a], Han Gil Na[b], Yong Jung Kwon[b], Hong Yeon Cho[b], Sung Yong Kang[b], Jae Young Park[c], Chongmu Lee[d], Myungho Kong[e] and Hyoun Woo Kim[b,*]

[a]*Department of Metallurgical & Materials Engineering, Inha Technical College, Incheon 402-752, Republic of Korea*
[b]*Division of Materials Science and Engineering, Hanyang University, Seoul 133-791, Republic of Korea*
[c]*Surface R&D Group, Korea Institute of Industrial Technology (KITEC), 156 Gaetbeol-ro, Yeonsu-gu, Incheon 406-840, Republic of Korea*
[d]*School of Materials Science and Engineering, Inha University, Incheon 402-751, Republic of Korea*
[e]*Department of Materials Engineering, Adama Science & Technology University, P. O. Box 1561, Adama, Ethiopia*

We decorated coated Gd_2O_3 nanoparticles on MgO nanowires by means of Gd sputtering and subsequent thermal annealing. The samples were characterized by X-ray diffraction, scanning electron microscope (SEM), and transmission electron microscopy. The surface roughness observed by SEM was revealed to be Gd_2O_3 nanoparticles in terms of TEM observation. The PL spectra exhibited a 2.9 eV-peak, which originated from the MgO nanowires, and thermal annealing produced green emission at about 2.4 eV, which is directly associated with the Gd_2O_3 structure. An additional weak peak at 2.0 eV was found to be related to impurities in the Gd_2O_3 structure.

Key words: MgO, Nanorwires, Gd_2O_3, Sputtering.

Introduction

Nanometer-scale structures have attracted considerable attention owing to their contribution to the understanding of basic concepts and their potential technological applications [1-23]. The addition of a shell layer to core nanowires has produced core-shell nanowires. It is expected that core-shell nanowires will exhibit improved or unique overall properties by combining the properties of individual components (e.g., core and shells).

Magnesium oxide (MgO) is a typical wide bandgap insulator [24-26] with its excellent thermodynamic stability, low dielectric constant, and low refractive index. MgO is an extremely important material with its application to catalysis, toxic waste remediation, and as an additive in refractory, paint, and superconductor products [27-29]. In particular, MgO nanowires possess a variety of extraordinary characteristics. They have the unique ability to pin magnetic flux lines within high-temperature flux lines [29, 30]. MgO nanowires have also been used as a template material for the epitaxial growth of thin films and nanowire arrays [30, 31]. Furthermore, the field emission properties of MgO nanowires have been reported [30]. Therefore, there is immense interest in preparing MgO 1D nanowires [29, 32-37].

In the present work, we prepared Gd-coated MgO nanowires and carried out thermal annealing. We found that Gd_2O_3 nanoparticles were generated on the stem MgO nanowires. Gadolinium oxide (Gd_2O_3) is a useful rare earth oxide, which has been extensively studied due to its optoelectronic, display, data storage, and sensor applications [38]. It has three polymorphic forms: hexagonal, monoclinic, and cubic [38]. Gd_2O_3 nanoparticles have attracted great attention due to their capacity to enhance imaging techniques such as Magnetic Resonance Imaging (MRI) [39]. Furthermore, it has controllable emission wavelengths through doping of a variety of lanthanide ions [40]. In the present work, we investigated a Gd_2O_3 nanoparticle-decorated sample in terms of its structural and optical properties.

Experimental

In a two-step process for preparing the core-shell structures, we first prepared the MgO nanowires by thermal evaporation of the pure MgB_2 powders in a quartz tube [41]. An alumina boat was inserted into a horizontal tube furnace and situated in the middle of a quartz tube. A piece of p-type (100) Si substrate was placed with the gold-coated side facing downwards. MgB_2 powders were evaporated to be deposited on the upper substrate. The furnace temperature was kept at 900°C for 2 h under a constant flow of carrier gas consisting of 97% Ar and 3% O_2. The total pressure was set to 2 Torr.

*Corresponding author:
Tel : +82-2-2220-0382
Fax: +82-2-2220-0389
E-mail: hyounwoo@hanyang.ac.kr

Physical sputtering on the as-prepared MgO nanowires was conducted using a DC turbo sputter coater (Emitech K575X, Emitech Ltd., Ashford, Kent, UK). During the sputtering process with a DC current of 80 mA, we carried out a sputter deposition with a circular Gd target at room temperature in high-purity (99.999%) argon (Ar) ambient. The vacuum chamber was evacuated to a base pressure of 2×10^2 Pa using a turbomolecular pump backed by a rotary pump. A sputtering deposition was carried out at a pressure of 2 Pa in high purity argon (Ar) gas (99.999%). Subsequently, the MgO-core/Gd-shell nanowires were heated to 500-900 °C for 1 h in O_2/Ar ambient.

The products were characterized by X-ray diffraction (XRD) (Philips X'pert MRD diffractometer with Cu$K\alpha_1$ radiation); field emission scanning electron microscopy (FE-SEM) (Hitachi, S-4200); and transmission electron microscopy (TEM) (Philips, CM-200) with energy dispersive X-ray spectroscopy (EDX) attached. Photoluminescence spectroscopy (PL) was measured at room temperature with a 325 nm line from a He-Cd laser (Kimon, 1K, Japan).

Results and Discussion

Fig. 1(a) shows the XRD pattern of the uncoated MgO nanowires, while Fig. 1(b) is that of the Gd-sputtered nanowires. Both the uncoated and coated samples exhibit diffraction peaks of the cubic structure of cubic MgO (JCPDS File No. 45-0946). For the coated sample, it is noteworthy that there are (002), (110), and (112) reflections of the hexagonal Gd structure with lattice constants at a = 0.3631 nm and c = 0.5777 nm (JCPDS: 89-2924). In addition, there are (321), (411), and (332) reflections of the cubic Gd_2O_3 structure with a lattice constant of a = 1. 0813 nm (JCPDS: 12-0797).

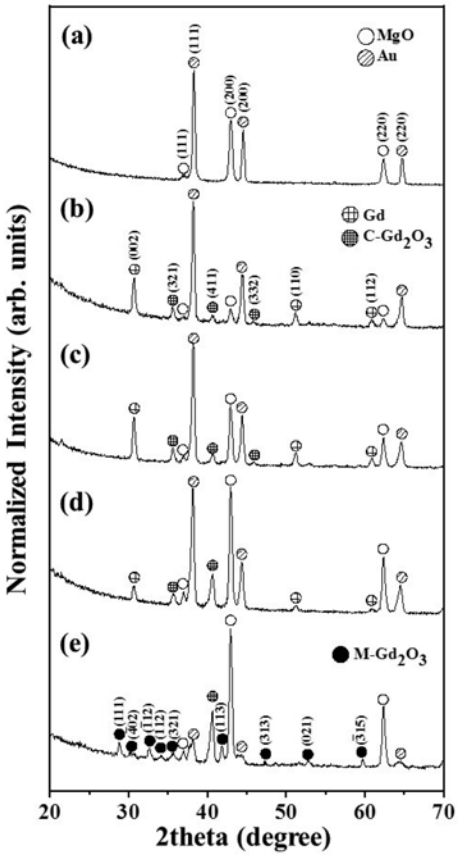

Fig. 1. XRD patterns of (a) pristine MgO nanowires, (b) sputtered MgO nanowires, and (c-e) core-shell nanowires annealed at (c) 500 °C, (d) 700 °C, (e) 900 °C.

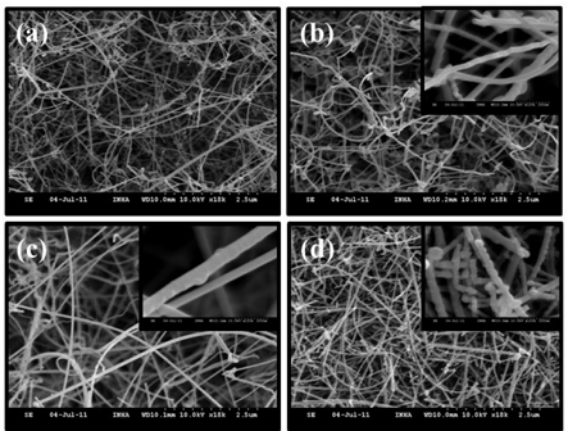

Fig. 2. SEM images of (a) pristine MgO nanowires and (b-d) core-shell nanowires annealed at (b) 500 °C, (c) 700 °C, (d) 900 °C.

We surmise that not only the Gd but also the Gd_2O_3 phase was generated by sputtering in an oxygen containing ambient.

Fig. 1(c), 1(d), and 1(e) shows the XRD spectra of the sputtered nanowires annealed at 500 °C, 700 °C, and 900 °C, respectively. The XRD patterns annealed at 500-700 °C are similar to those of the as-sputtered ones, being comprised of reflections of the cubic MgO, cubic Au, hexagonal Gd, and cubic Gd_2O_3 phases. On the other hand, Fig. 1(e) reveals that the XRD pattern of the 900 °C-annealed sample exhibits several peaks of the monoclinic Gd_2O_3 structure (JCPDS: 42-1465) in addition to the cubic MgO, cubic Au, hexagonal Gd, and cubic Gd_2O_3 phases. We reveal that the cubic Gd_2O_3 structures have been transformed to monoclinic Gd_2O_3 structures at a higher temperature of 900 °C.

Fig. 2(a) shows a SEM image of the pristine MgO nanowires, while Fig. 2(b), 2(c), and 2(d) shows those of the annealed core-shell nanowires at 500, 700, and 900 °C, respectively. All the samples exhibited 1D morphology, regardless of thermal annealing. The upper-right inset of Fig. 2(b) shows that the 500 °C-annealed sample has a rough surface. It is noteworthy that the surface roughness of the nanowire tends to increase with increasing annealing temperature, exhibiting the agglomerated nature of the Pt nanoparticles at 900 °C.

In order to investigate the structure and crystallinity of the Pt nanoparticle-decorated branched nanowires,

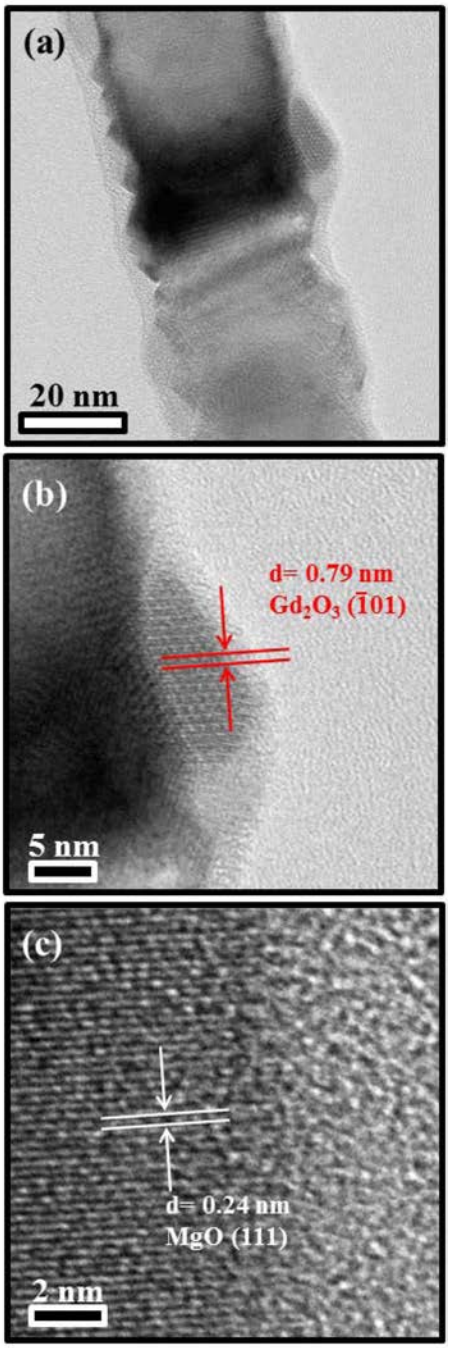

Fig. 3. (a) TEM image of the core-shell nanowires annealed at 900 °C. (b) Enlarged TEM image of the surface nanoparticles. (c) Lattice-resolved TEM image of the core MgO nanowires.

we performed a TEM analysis. Fig. 3(a) shows a low-magnification TEM image, and Fig. 3(b) is the corresponding enlarged image. The resolved spacing between the parallel fringes is about 0.79 nm, corresponding to the (101) lattice plane of the monoclinic Gd_2O_3. The lattice-resolved image reveals that the stem part is comprised of a cubic MgO structure (Fig. 3(c)).

Fig. 4(c) shows a typical TEM image of a 900 °C-annealed nanowire, while Fig. 4(b), 4(c), and 4(d) are the

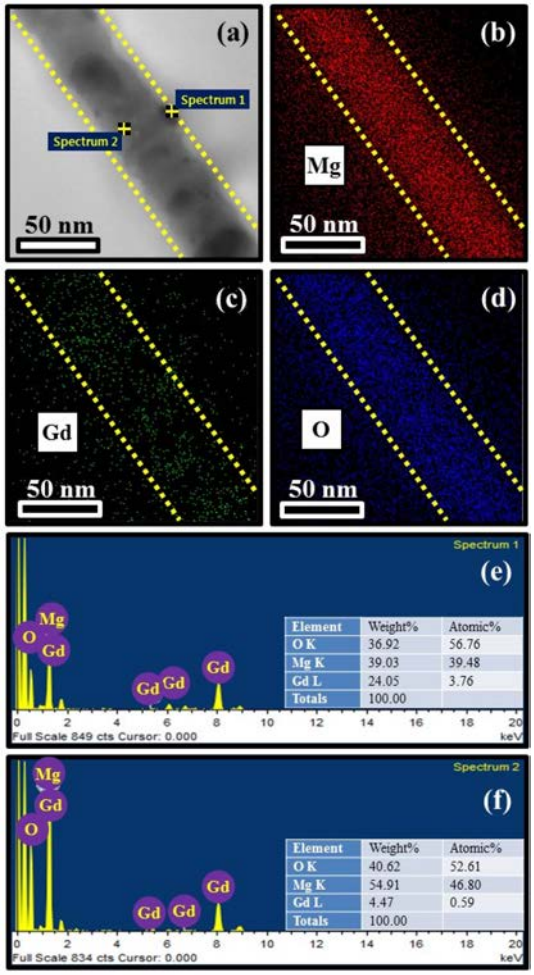

Fig. 4. (a) Typical TEM image and EDX elemental maps for the (b) Mg, (c) Gd, and (d) O elements. EDX spectrum taken from the (e) nanoparticle region and (f) stem region of the 900 °C-annealed composite nanowires.

elemental maps of the Mg, Gd, and O elements, respectively, indicating the presence of these elements. Fig. 4(e) and 4(f) shows the EDX spectra of the particle and stem region of the nanowires in Fig. 4(a). The atomic percentages of the Gd element of the particle and stem region of the nanowires were 3.76 and 0.59%, respectively.

In order to investigate the optical properties, we carried out a PL analysis. To investigate the PL properties in more detail, a Gaussian fitting analysis was performed. Fig. 5(a) shows the PL spectrum of the pristine MgO nanowires, exhibiting a main peak at around 2.85 eV. A similar blue peak at 2.81-2.84 has been previously observed from MgO nanowires [42, 43], MgO branched nanostructures [44], MgO nanowires [42], and MgO nanoplates [45]. It is well recognized that the blue emissions originate from defects in MgO, such as oxygen vacancies [25, 44, 45].

In Fig. 5(c), we observe that there is a weak peak at 2.4 eV. By increasing the annealing temperature up to 700-900 °C, the relative intensity of the 2.4 eV-peak

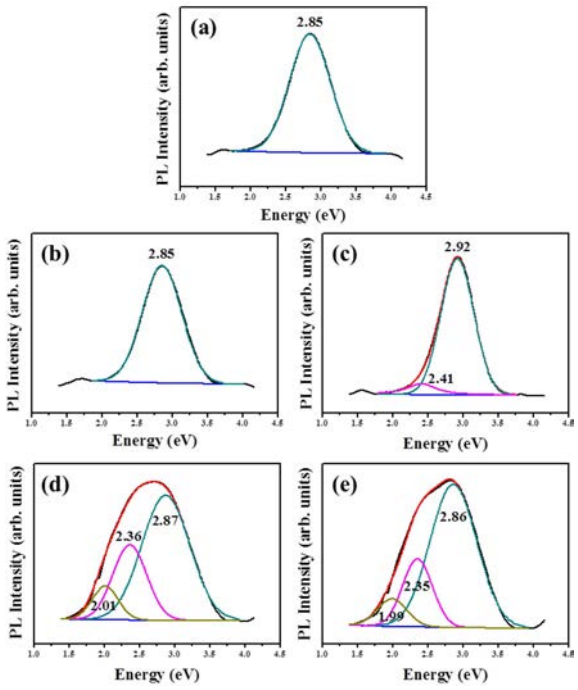

Fig. 5. Normalized PL spectra of the (a) uncoated and (b-e) coated MgO nanowires. The sample (b) was not annealed, while those at (c) 500 °C, (d) 700 °C, and (e) 900 °C were annealed. The PL spectra exhibited a three-peak Gaussian fitting.

was significantly increased. Furthermore, at 700-900 °C, a weak peak at around 2.0 eV appeared in the PL spectra (Figs. 5(d)-(e)).

The emission at 2.4 eV is related to the generation of the Gd_2O_3 phase. Goldys et al. reported that the PL spectrum of the Gd_2O_3 nanoparticles synthesized by the hydrogen flame pyrolysis method [46] exhibited a broad emission peak at 2.4 eV.

However, it is not clear what the exact origin of the weak 2.0 eV-peak is. Previous work has reported the appearance of a 2.0 eV-peak from the Eu-doped Gd_2O_3 nanoparticles [46, 47]. It is possible that the 2.0 2V-peak in the present study is associated with the impurities in the Gd_2O_3 nanoparticles.

In the present study, the results show that a high-temperature fabrication process can include various impurities from the ambient and/or furnace, contributing to the observed emissions. However, further detailed study is necessary.

Conclusions

In summary, we have sputtered MgO nanowires with a Gd sputtering target for the first time. Subsequent thermal annealing produced Gd_2O_3 nanoparticles. The XRD patterns revealed that annealing at 500-700 °C produced a cubic Gd_2O_3 structure, whereas the nanoparticles annealed at 900 °C corresponded to the phase of the monoclinic Gd_2O_3. SEM images indicate that the surface roughness of the nanowires increases with increasing annealing temperature. TEM analysis confirms that the nanoparticles of the 900 °C-annealed nanowires exhibit a monoclinic Gd_2O_3 structure. TEM-EDX elemental maps confirmed the presence of Gd in addition to Mg and O elements. The PL spectra exhibited a blue peak at 2.9 eV. The thermal annealing produced a green emission at about 2.4 eV, which is directly related to the Gd_2O_3 structure. The weak peak at 2.0 eV resulting from the 900C-annealing is likely to be associated with impurities in the Gd_2O_3 structure. This finding contributes to potential applications of coaxial 1D nanostructures to a variety of future nanodevices.

Acknowledgments

This work was supported by a National Research Foundation of Korea (NRF) grant funded by the Korean government (MEST) (No. NRF-2013R1A2A 2A01068438).

References

1. A.P. Alivisatos, Science 271 (1996) 933-937.
2. X. Duan, Y. Huang, Y. Cui, J. Wang and C. M. Lieber, Nature 409 (2001) 66-69.
3. W. A. de Heer, A. Chatelain and D. Ugarte, Science 270 (1995) 1179-1180.
4. R. Kuar, M. C. Mishra, B. K. Sharma, V. Vyas and G. Sharma, Electron. Mater. Lett. 9 (2013) 19-23.
5. H.-W. Cui, D.-S. Li and Q. Fan, Electron. Mater. Lett. 9 (2013) 1-5.
6. M. A. Majeed Khan, W. Khan, M. Ahamed, M. S. Alsalhi and T. Ahmed, Electron. Mater. Lett. 9 (2013) 53-57.
7. R. Sabbaghizadeh and M. Hashim, Electron. Mater. Lett. 9 (2013) 115-118.
8. D. Soundararajan, Y. Lim, M.-P. Chen and K. H. Kim, Electron. Mater. Lett. 9 (2013) 177-182.
9. T. Prakash, S. Ramasamy and B. S. Murty, Electron. Mater. Lett. 9 (2013) 207-211.
10. A. Mondal, J. C. Dhar, P. Chinnamuthu, N. K. Singh, K. K. Chattopadhay, S. K. Das, S. Ch Das and A. Bhattachayya, Electron. Mater. Lett. 9 (2013) 213-217.
11. S. N. Heo, K. Y. Park, Y. J. Seo, F. Ahmed, M. S. Anwar and B. H. Koo, Electron. Mater. Lett. 9 (2013) 261-265.
12. S. Sharma and S. Chawla, Electron. Mater. Lett. 9 (2013) 267-271.
13. K. Seo, M. Suh and S. Ju, Electron. Mater. Lett. 9 (2013) 273-277.
14. C.-H. Lee, D.-J. Choi and Y.-J. Oh, Electron. Mater. Lett. 9 (2013) 283-286.
15. Y. Jia, F. Yang, F. Cai, C. Cheng and Y. Zhao, Electron. Mater. Lett. 9 (2013) 287-291.
16. S. Kim, G. Nam, K. G. Yim, J. Lee, Y. Kim and J.-Y. Leem, Electron. Mater. Lett. 9 (2013) 293-298.
17. H.-W. Cui, D.-S. Li and Q. Fan, Electron. Mater. Lett. 9 (2013) 299-307.
18. H. Lee, J.-H. Shin, J. Chae, J. B. Kim, T.-H. Kim and K.-B. Park, Electron. Mater. Lett. 9 (2013) 357-362.
19. S. Kumar, P. Dharma and V. Sharma, Electron. Mater. Lett. 9 (2013) 371-374.

20. T. Sreesattabud, B. J. Gibbons, A. Watcharapasom and S. Jiansirisomboon, Electron. Mater. Lett. 9 (2013) 409-412.
21. N.-M. Park, J. Shin, B. Kim, K. H. Kim and W.-S. Cheong, Electron. Mater. Lett. 9 (2013) 467-469.
22. C.-G. Kuo, H. Chang, L.-R. Hwang, S. Hor, J.-S. Chen, G.-Y. Liu and S.-C. Cheng, Electron. Mater. Lett. 9 (2013) 481-484.
23. J. Huang, S. Somu and A. Busnaina, Electron. Mater. Lett. 9 (2013) 505-507.
24. G. P. Summers, T. M. Wilson, B. T. Jeffries, H. T. Tohver, Y. Chen and M. M. Abraham, Phys. Rev. B 27 (1983) 1283-1291.
25. G. H. Rosenblatt, M. W. Rowe, G. P. Williams, Jr., R. T. Williams and Y. Chen, Phys. Rev. B 39 (1989) 10309-10318.
26. J. L. Grant, R. Cooper, P. Zeglinski and J. F. Boas, J. Chem. Phys. 90 (1989) 807-812.
27. S. H. C. Liang and I. D. Gay, J. Catal. 101 (1986) 293-300.
28. A. N. Copp, Am. Ceram. Soc. Bull. 74 (1995) 135-137.
29. P. Yang and C. M. Lieber, Science 273 (1996) 1836-1840.
30. L. A. Ma, Z. X. Lin, J. Y. Lin, Y. A. Zhang, L. Q. Hu and T. L. Guo, Physica E 41 (2009) 1500-1503.
31. K. Nagashima, T. Yanagida, H. Tanaka, S. Seki, A. Saeki, S. Tagawa and T. Kawai, J. Am. Chem. Soc. 130 (2008) 5378-5382.
32. Y. Q. Zhu, W. K. Hsu, W. Z. Zhou, M. Terrones, H. W. Kroto and D. R. M. Walton, Chem. Phys. Lett. 347 (2001) 337-343.
33. Y. Li, Y. Bando and T. Sato, Chem. Phys. Lett. 359 (2002) 141-145.
34. Y. Yin, G. Zhang and Y. Xia, Adv. Funct. Mater. 12 (2002) 293-298.
35. J. Zhang, L. Zhang, X. Peng and X. Wang, Appl. Phys. A 73 (2001) 773-775.
36. K. L. Klug and V. P. Dravid, Appl. Phys. Lett. 81 (2002) 1687-1689.
37. P. Yang and C. M. Lieber, J. Mater. Res. 12 (1997) 2981-2996.
38. N. Dhananjaya, H. Nagabhushana, B. M. Nagabhushana, B. Rudraswamy, S. C. Sharma, D. V. Sunitha, C. Shivakumara and R. P. S. Chakradhar, Spectrochim. Acta A 96 (2012) 532-540.
39. A. T. M. A. Rahman, K. Vasilev and P. Majewski, J. Colloid Interf. Sci. 354 (2011) 592-596.
40. J. H. Kim, Y. K. Jung and J.-K. Lee, J. Nanopart. Res. 13 (2011) 2311-2318.
41. H. W. Kim, N. H. Kim, J. H. Myung and S. H. Shim, Phys. Stat. Sol. (a) 202 (2005) 1758-1762.
42. F. L. Deepak, P. Saldanha, S. R. C. Vivekchand and A. Govindaraj, Chem. Phys. Lett. 417 (2006) 535-539.
43. H. W. Kim and S. H. Shim, Chem. Phys. Lett. 422 (2006) 165-169.
44. Y. Hao, G. Meng, C. Ye, X. Zhang and L. Zhang, J. Phys. Chem. B 109 (2005) 11204-11208.
45. H. Niu, Q. Yang, K. Tang and Y. Xie, Micropor. Mesopor. Mat. 96 (2006) 428-433.
46. E. M. Goldys, K. Drozdowicz-Yomsia, S. Jinjun, D. Dosev, I. M. Kennedy, S. Yatsunenko and M. Godlewski, J. Am. Chem. Soc. 128 (2006) 14498-14505.
47. H. Chen, C. He, C. Gao, Y. Ma, J. Zhang, X. Wang, S. Gao, D. Li, S. Kan and G. Zou, J. Phys.: Condens. Matter. 19 (2007) 425229.